

CHAPTER 107

HYDRODYNAMIC FORCES ON BOTTOM-SEATED HEMISPHERE IN WAVES AND CURRENTS

H. Nishida¹, A. Tada² and F. Nishihira³

Abstract

The characteristics of hydrodynamic forces acting on a bottom-seated hemisphere in waves only, in currents only and in waves & currents are presented from the viewpoint of the design of an artificial reef. A large number of regular wave experiments were conducted in order to find the empirical formulas of the hydrodynamic coefficients for the bottom-seated hemisphere. It is shown that the proposed empirical formulas are sufficiently accurate for predicting the hydrodynamic forces. The effects of the normalized water depth and hemisphere spacing relative to its diameter are also elucidated experimentally.

Introduction

In order to provide a continued supply of marine products, the Japanese fishing industry has been shifting from fish catching to fish farming. Various artificial reefs have been used to attract fish by producing coherent eddies with upward flow as well as by providing hiding places for fish. Most of these reefs have rectangular shapes and caused tearing of fishing nets. In order to reduce entanglement of fishing nets, the authors have proposed bottom-seated hemispherical reefs. For the design of such a reef against waves and currents, the hydrodynamic forces acting on the reef need to be predicted.

=====
¹ Research Engineer, Technical Research Institute, Nishimatsu Construction Co., Ltd., 2570-4, Shimotsuruma, Yamato, Kanagawa 242, Japan

² Senior Research Engineer, Technical Research Institute, Nishimatsu Construction Co., Ltd., 2570-4, Shimotsuruma, Yamato, Kanagawa 242, Japan

³ Dr. and General Manager, Technical Research Institute, Nishimatsu Construction Co., Ltd., 2570-4, Shimotsuruma, Yamato, Kanagawa 242, Japan

Hydraulic Experiments

Regular wave experiments were conducted in a wave flume which was 65m long, 1.0 m wide and 1.6 m high. The flume was capable of generating steady currents in both directions relative to the direction of wave propagation. As a first attempt, plastic hemispheres without any opening were used in the experiments. The experimental results presented herein may hence be of interest to researchers working on the design of quarry stone armor units. The three-dimensional hydrodynamic force acting on an individual hemisphere was measured using a three-component waterproof load cell with a water pressure adjustment. Fluid velocities at the location of the hemisphere were measured using a two-component electromagnetic current meter. Free surface oscillations above the hemisphere are measured using a capacitance wave gage. For limited tests, flow visualization was performed to examine the flow pattern and eddy formation using a laser and a high speed camera, as shown in Photo.1. A large number of tests were performed for a single hemisphere and three hemispheres in a row.

Fig.1 shows the experimental setup for three hemispheres, where X =horizontal coordinate taken to be positive in the direction of wave propagation with $X=0$ at the center of the middle hemisphere; Z =vertical coordinate taken to be positive upward with $Z=0$ at the still water level(SWL); h =water depth below SWL; H =height of incident regular waves whose period is denoted by T ; D =diameter of the hemisphere; and L_f =distance between the centers of two adjacent hemispheres. The experiments were conducted for the following conditions;

- 1) $h=40,60$ and 80 cm
- 2) $H=3.0,6.0$ and 9.0 cm
- 3) $T=1.2,1.6,2.0,2.4$ and 2.8 sec
- 4) $D=15.0$ and 20.0 cm
- 5) $L_f/D=1.0,1.5,2.0,2.5$ and 3.0
- 6) $U=\pm 5.0, \pm 10.0, \pm 20.0, \pm 30.0$ and ± 40.0 cm/sec

where U =depth-averaged steady current velocity which is negative for opposing currents.

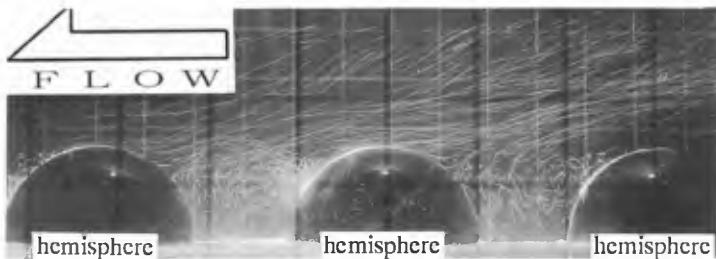


Photo.1 An example of flow visualization in currents only

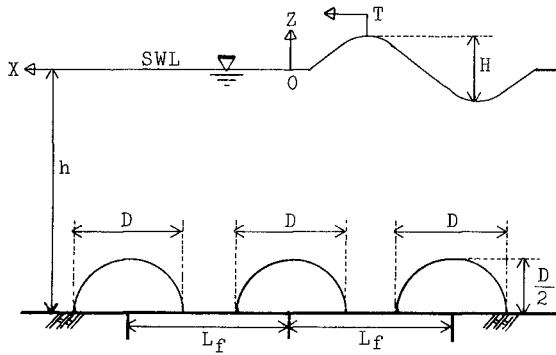


Fig.1 Experimental setup for three hemispheres

Data Analysis

The measured horizontal and vertical hydrodynamic forces acting on the hemisphere are assumed to be expressed in the form proposed by Morison (Morison et al. 1950).

$$F_x = \frac{1}{2} \rho C_D \left(\frac{\pi D^2}{8} \right) (u + U) |u + U| + \rho C_M \left(\frac{\pi D^3}{12} \right) \frac{du}{dt} \quad (1)$$

$$F_{z_M} = \frac{1}{2} \rho C_L \left(\frac{\pi D^2}{8} \right) (u_m + U)^2 \quad (2)$$

where F_x = horizontal force ; ρ = fluid density ; u = oscillatory horizontal fluid velocity ; U = steady fluid velocity ; C_D = drag coefficient ; C_M = inertia coefficient ; and C_L = lift coefficient .The velocities u and U are at the location of the hemisphere. The constant values of C_D and C_M for each test were determined using the method of least squares (Reid 1957). The constant value of C_L was estimated such that the maximum vertical force F_{z_M} could be predicted by Eq.(2) accurately. This was because Eq.(2) with constant C_L did not reproduce the entire variation of F_z with respect to time t very well.

Drag, Inertia and Lift Coefficients

The efforts for developing the empirical relationships for C_D , C_M and C_L were separated into;

- single hemisphere in waves only
- single hemisphere in currents only
- single hemisphere in waves & currents
- middle hemisphere among three hemispheres in waves only
- middle hemisphere among three hemispheres in currents only

For these tests, the inertia force was generally dominant in Eq.(1) and the horizontal force was normally greater than the vertical force. In addition, it was judged that there was little scale effect on hemispherical models because the influence of Reynolds number $Re=u_m D/\nu$ on the wave force coefficients were negligible under adopted experimental conditions, refer to Figs.2 and 3.

Fig.4 shows the relationship between the wave force coefficients and Keulegan-Carpenter number($K.C.=u_m T/D$) for the single hemisphere in the water depth of 40 cm, where u_m is the maximum value of u . As shown in Fig.4, C_M in waves only is on the order of 1.35 and C_D in waves only varies with $K.C.$ in a manner similar to a sphere (Jenkins and Inman 1976).

Eqs.(3), (4) and (5) are the empirical formulas of C_D , C_M and C_L in waves only, respectively. They are statistically derived by means of the method of least squares.

$$C_D = 6.79 \cdot (K.C.)^{-0.89} \quad \text{for } U=0 \quad (3)$$

$$C_M = 1.35 \quad \text{for } U=0 \quad (4)$$

$$C_L = 3.3 \cdot (K.C.)^{-0.98} \quad \text{for } U=0 \quad (5)$$

Eqs.(6) and (7) are the empirical formulas of the drag and lift coefficients in currents only for the single hemisphere in the depth of 40 cm, respectively. The effect of Reynolds number $Re=UD/\nu$ on these coefficients seems to be also negligible for the case of currents only as shown in Fig.5.

$$C_D = 0.48 \quad \text{for } u_m=0 \quad (6)$$

$$C_L = 0.8 \quad \text{for } u_m=0 \quad (7)$$

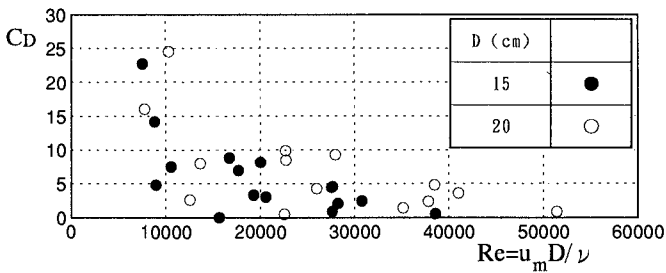


Fig.2 Drag coefficient C_D versus $Re(=u_m D/\nu)$ in waves only

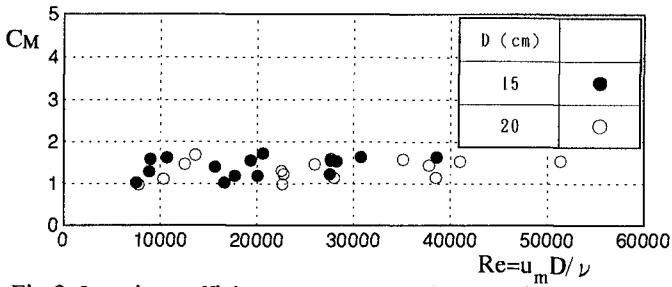


Fig.3 Inertia coefficient C_M versus $Re(=u_m D/\nu)$ in waves only

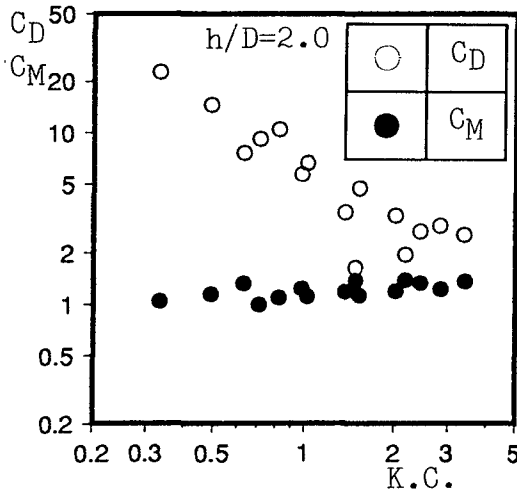


Fig.4 Drag coefficient C_D , inertia coefficient C_M versus $K.C.$ in waves only

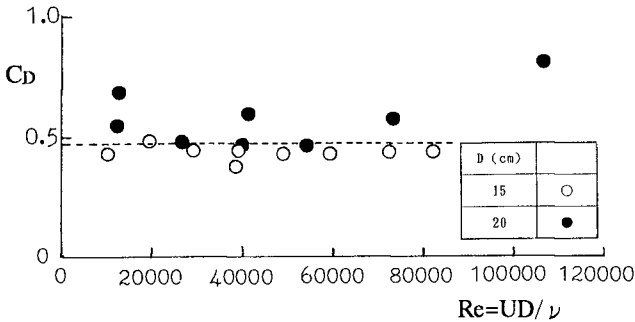


Fig.5 Drag coefficient C_D versus $Re(=UD/\nu)$ in currents only

Fig.6 shows the relationship between C_D in waves & currents and the modified Keulegan-Carpenter number $K=(|U|+u_m)T/D$ for the single hemisphere in fair currents for which $U>0$ (Iwagaki et al . 1983). The water depth is 40 cm. The parameter α shown in the figure is defined as $\alpha=|U|/u_m$ and two solid lines in this figure indicate the empirical formulas of C_D in waves only [Eq.(3)] and in currents only [Eq.(6)] , respectively. C_D is slightly affected by K and α and also approximately approaches 0.48 for large α , corresponding to the value of C_D for currents only.

On the basis of these characteristics shown in Fig.6, the following empirical formula of C_D for the single hemisphere in waves & currents with $U>0$ have been proposed;

$$C_D = 6.97 \cdot e^{-\beta} \cdot K^{-0.89} + 0.48(1 - e^{-\beta}) \text{ for } U>0 \quad (8)$$

with $\beta = 0.019\alpha^2 + 0.99\alpha - 0.07$

When α is equal to zero and $K=K.C.$, Eq.(8) yields almost the same value of C_D in waves only. On the other hand, this formula corresponds to C_D in currents only when α tends to infinity. The broken lines in Fig.6 indicate Eq.(8) for α in the range of 0.25 to 2.5. In order to evaluate the accuracy of Eq.(8), Fig.7 compares C_D calculated by Eq.(8) with C_D obtained from the experiments. It is realized that the former agrees fairly with the latter, regardless of α .

Fig.8, for the case of water depth 40 cm, shows the relationship between the inertia coefficient in waves & currents and K for the single hemisphere in fair currents. It is obvious that C_M increases with increasing K in the region $C_M>1.35$, whereas C_M decreases with increasing K in the region $C_M<1.35$. Furthermore , C_M decreases with increasing α if K is assumed to be constant.

Considering the above characteristics, the following empirical formula of C_M as a function of α and K is derived from the method of least squares.

$$C_M = 1.35 \cdot \exp \left[0.084(1.18 - \alpha)K \right] \text{ for } U>0 \quad (9)$$

Eq.(9) is equivalent to C_M in waves only if α is equal to 1.18. Broken lines in Fig.8 indicate the above formula for α in the range of 0.25 to 3.5. It is found that Eq.(9) coincides fairly with the experimental values.

The relationship between C_M calculated by Eq.(9) and C_M obtained from the experimental results is also shown in Fig.9. The reason why the accuracy of Eq.(9) is lower as the parameter α becomes larger is that the drag force is more predominant than the inertia force and it is hard to estimate C_M accurately for large α .

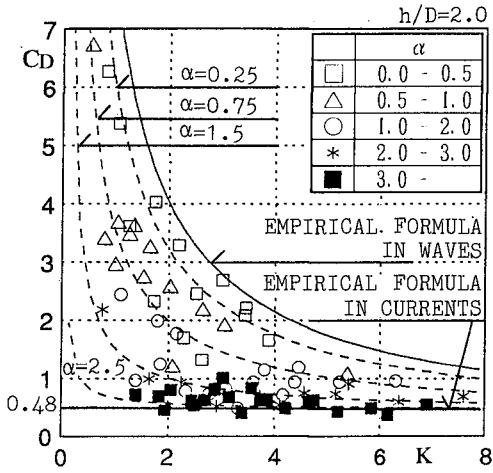


Fig.6 Drag coefficient C_D versus K in waves & currents(fair current)

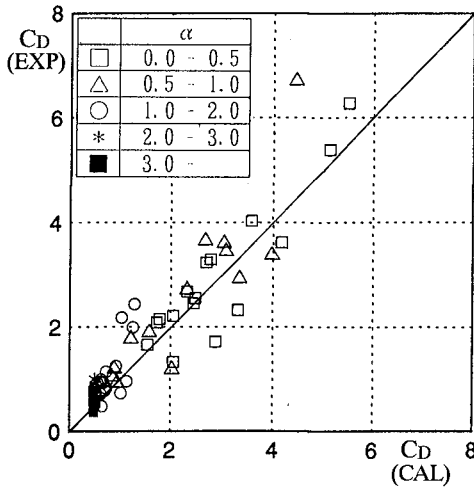


Fig.7 Drag coefficient C_D (EXP) versus Drag coefficient C_D (CAL)

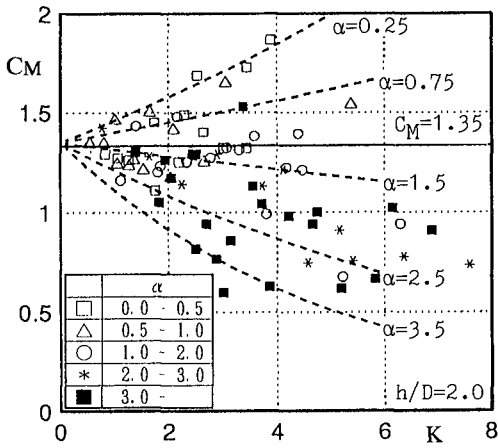


Fig.8 Inertia coefficient C_M versus K in waves & currents(fair current)

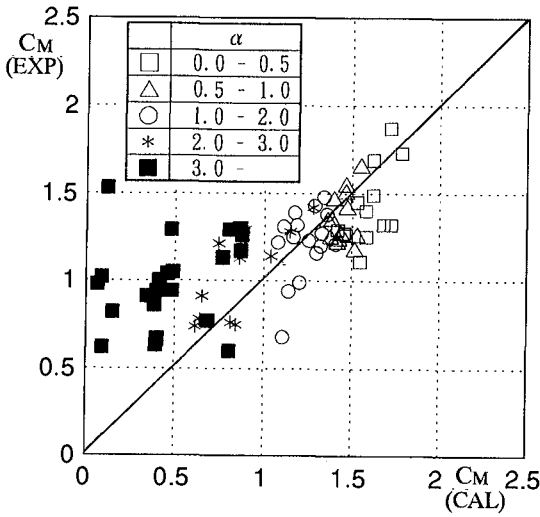


Fig.9 Inertia coefficient C_M (EXP) versus inertia coefficient C_M (CAL)

Fig.10 shows the relationship between C_L in waves & currents and K for the single hemisphere in the water depth of 40 cm . The variations of C_L with respect to these dimensionless parameters were similar to those associated with C_D . The following formula in fair currents is introduced.

$$C_L = 3.3 \cdot e^{-0.5\alpha} \cdot K^{-0.98} + 0.8(1 - e^{-0.5\alpha})^{0.16} \text{ for } U > 0 \quad (10)$$

The relationships between the hydrodynamic coefficients and K for the single hemisphere in adverse currents for which $U < 0$ and α are shown in Figs.11 and 12. Moreover, the following empirical formulas for adverse currents are derived using the same procedure .

$$C_D = 6.97 \cdot e^{-\beta} \cdot K^{-0.89} + 0.48(1 - e^{-\beta}) \text{ for } U < 0 \quad (11)$$

$$\text{with } \beta = -0.08\alpha^2 + 1.05\alpha - 0.1$$

$$C_M = 1.35 \cdot \exp \left[0.063(1.34 - \alpha)K \right] \text{ for } U < 0 \quad (12)$$

$$C_L = 3.3 \cdot e^{-0.6\alpha} \cdot K^{-0.98} + 0.8(1 - e^{-0.6\alpha})^{0.43} \text{ for } U < 0 \quad (13)$$

Those formulas should be reevaluated because free surface oscillations became larger and more irregular as waves propagated over a long distance in adverse currents.

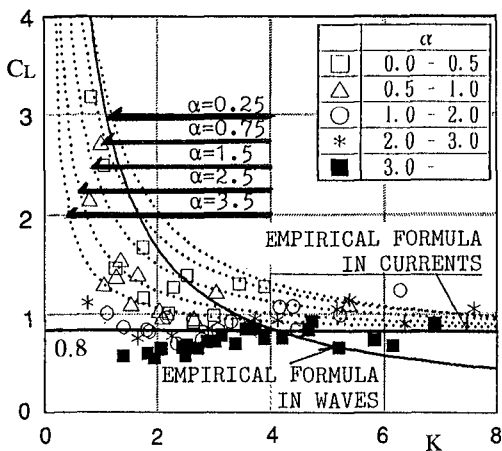


Fig.10 Lift coefficient C_L versus K in waves & currents(fair current)

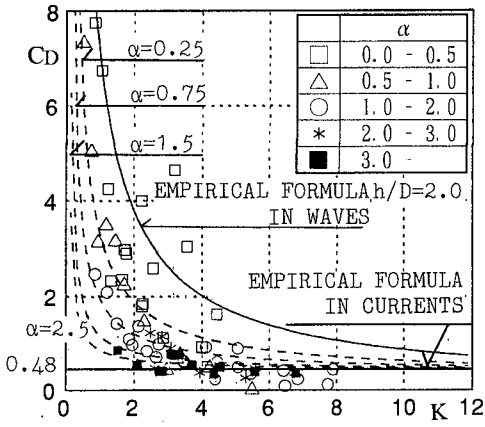


Fig.11 Drag coefficient C_D versus K in waves & current(adverse current)

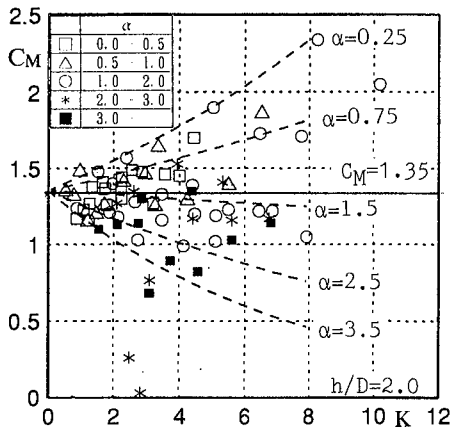


Fig.12 Inertia coefficient C_M versus K in waves & currents(adverse current)

Applicability of Empirical Formulas

The above experimental results were for the water depth of 40cm. It is very important to study the effect of the variation of water depth on C_D and C_M in waves & currents. Figs.13 and 14 show the effects of the water depth normalized by the diameter D on C_D and C_M , respectively. These coefficients are almost constant, regardless of the dimensionless parameter h/D . In other words, C_D and C_M in waves & currents are not practically affected by the effect of the water depth in the range $h/D=2.0\sim 4.0$ tested here.

Fig.15 shows the relationship between the dimensionless C_{MG}/C_M and L_f/D , where C_{MG} is the inertia coefficient of the middle hemisphere among three hemispheres and L_f is defined in Fig.1. C_{MG}/C_M approximately approaches 1 for large L_f/D . The empirical formulas on the inertia coefficient proposed in this paper are valid for the range $L_f/D>2.0$. The effect of the adjacent hemispheres on the drag coefficient was also negligible for $L_f/D>2.0$.

Conclusions

The experimental results in this paper are summarized as follows;

- (1)The empirical formulas of C_D and C_M in waves & currents are derived using the modified Keulegan-Carpenter number K and the parameter α indicating the current strength relative to the wave velocity. These formulas are accurate enough to estimate the hydrodynamic forces.
- (2)These hydrodynamic coefficients in waves & currents are not affected by the normalized water depth h/D in the range $h/D=2.0\sim 4.0$.
- (3)The empirical formulas proposed in this study are valid for the range $L_f/D>2.0$ for the conditions shown in Fig.1.

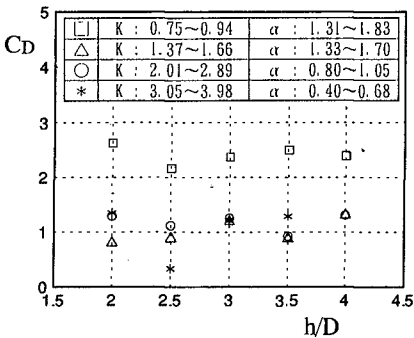


Fig.13 Drag coefficient C_D versus h/D

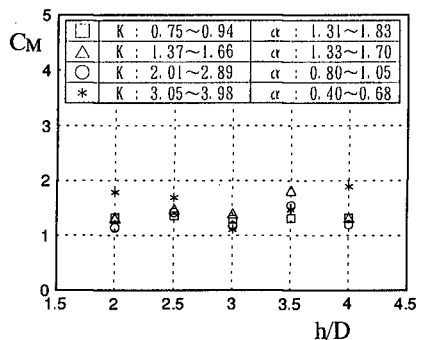


Fig.14 Inertia coefficient C_M versus h/D

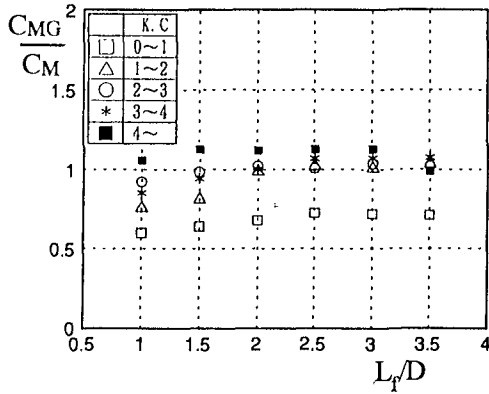


Fig.15 C_{MG}/C_M versus L_f/D

Acknowledgment

The authors would like to express their gratitude to Prof. Nobuhisa Kobayasi at the University of Delaware, whose insight and guidance were of great assistance in the preparation of this manuscript.

References

Iwagaki, Y., T. Asano and F. Nagai(1983)"Hydrodynamic forces on a circular cylinder placed in waves-current co-existing fields", Mem. Fac. Eng., Kyoto Univ., Vol.45, No.1, 11-23.

Jenkins, S.A. and Inman, D.L. (1976). "Forces on a sphere undere linear progressive waves ",Proc., 15th Int. Conf. on Coastal Eng., ASCE, 2413-2428.

Keulegan,G.H. and Carpenter, L.H.(1958). "Forces on cylinders and plates in an oscillating fluid." J. Res. Nat. Bur. Standards, 60(5), 423-440.

Morison ,J.R.,et al.(1950)."The forces exerted by surface waves on piles." Petroleum Trans., AIME, 189, 149-157.

Reid,R.O.(1957). "Correlation of water level variations with wave forces on a vertical pile for non-periodic waves." Proc., 6th Int. Conf. Coastal Eng., ASCE, 749-786.